

Ultimate strength design of thin-wall circular bridge piers

Autor(en): **Warner, R.F. / Brettle, H.J.**

Objektyp: **Article**

Zeitschrift: **IABSE publications = Mémoires AIPC = IVBH Abhandlungen**

Band (Jahr): **27 (1967)**

PDF erstellt am: **18.09.2024**

Persistenter Link: <https://doi.org/10.5169/seals-21551>

Nutzungsbedingungen

Die ETH-Bibliothek ist Anbieterin der digitalisierten Zeitschriften. Sie besitzt keine Urheberrechte an den Inhalten der Zeitschriften. Die Rechte liegen in der Regel bei den Herausgebern.

Die auf der Plattform e-periodica veröffentlichten Dokumente stehen für nicht-kommerzielle Zwecke in Lehre und Forschung sowie für die private Nutzung frei zur Verfügung. Einzelne Dateien oder Ausdrucke aus diesem Angebot können zusammen mit diesen Nutzungsbedingungen und den korrekten Herkunftsbezeichnungen weitergegeben werden.

Das Veröffentlichen von Bildern in Print- und Online-Publikationen ist nur mit vorheriger Genehmigung der Rechteinhaber erlaubt. Die systematische Speicherung von Teilen des elektronischen Angebots auf anderen Servern bedarf ebenfalls des schriftlichen Einverständnisses der Rechteinhaber.

Haftungsausschluss

Alle Angaben erfolgen ohne Gewähr für Vollständigkeit oder Richtigkeit. Es wird keine Haftung übernommen für Schäden durch die Verwendung von Informationen aus diesem Online-Angebot oder durch das Fehlen von Informationen. Dies gilt auch für Inhalte Dritter, die über dieses Angebot zugänglich sind.

Ultimate Strength Design of Thin-Wall Circular Bridge Piers

Calcul à la limite des piles de pont circulaires à parois minces

*Bemessung dünnwandiger, kreisförmiger Brückenpfeiler
nach dem Traglastverfahren*

R. F. WARNER

H. J. BRETTLER

School of Civil Engineering, University of New South Wales, Sydney

1. Introduction

In normal circumstances bridge piers are subjected to sustained compressive dead load forces and intermittent horizontal and vertical live load forces which cause additional compression, in conjunction with bending moments about axes parallel to and perpendicular to the bridge centre line. Use of circular cross-sections for bridge piers simplifies the analysis of bi-axial bending, while use of thin-wall circular sections results in a very considerable saving in material over both solid circular and solid rectangular sections. The thin-wall circular section is particularly appropriate when the transverse and longitudinal moments are of the same order of magnitude. Hollow circular piers can be cast rapidly and economically "in-situ" using modern construction methods, such as the slip-form technique [1], so that savings in material may often more than compensate for the additional construction costs.

The only readily available method of analysis and design of thin-wall circular reinforced concrete members is contained in ACI Standard 505-44, "Specification for the Design and Construction of Reinforced Concrete Chimneys" [2]. In this code, equations based on elastic theory are derived for the stresses in reinforced concrete chimneys subjected to dead load and horizontal wind load.

It has however long been recognized that, in reinforced concrete compression members, stresses computed on the assumption of elastic behaviour bear little resemblance to those actually occurring, even under normal working loads. The choice of appropriate allowable stresses is thus particularly difficult

for compression members. Indeed, most so-called allowable stress methods of design for reinforced concrete compression members are today based on considerations of ultimate strength [3].

In the present paper, ultimate strength equations are derived for thin-wall circular sections subjected to combined axial compression and bending moment. Design charts have been prepared from these equations, and are included to facilitate calculations for ultimate strength analysis and design.

Several of the simplifying assumptions made in this study have also been made in the elastic analysis contained in Reference 2. In particular, it is assumed that the wall-thickness t is small compared with the mean radius r , and that the reinforcing steel may be replaced by a continuous steel shell of equivalent area, located on the mean circumference of the concrete shell.

2. Notation

A, B, C, D	non-dimensional trigonometric functions defined in Eqs. (25) to (28).
A_c	total concrete area in cross-section.
A_s	total steel area in cross-section.
e	eccentricity of compressive force N .
e_c	concrete strain.
e'_c	concrete strain at maximum stress f'_c in control test.
e_{cu}	concrete compressive strain at upper extreme fibre in section at ultimate load.
e_s	steel strain.
e_{s2}	tensile steel strain at lower extreme fibre in section at ultimate load.
e_{sy}	steel yield strain.
f_c	concrete stress.
f_{ca}	allowable concrete compressive stress for elastic analysis.
f_{cw}	maximum concrete compressive stress in elastic analysis.
f'_c	maximum concrete stress obtained from control test.
f_s	steel stress.
f_{sa}	allowable steel stress for elastic analysis.
f_{sw}	maximum steel tensile stress in elastic analysis.
f_{sy}	steel yield stress.
k	ratio of assumed maximum concrete stress in the pier section at failure to control test strength f'_c .
M	resultant bending moment acting on section.
N	compressive force acting on section.
p	proportion of steel reinforcement; $p = A_s/A_c$.
P	total compressive force in concrete above the neutral axis.
\bar{P}	non-dimensionalized form for P .
P'	moment of P about the neutral axis.

\bar{P}'	non-dimensionalized form for P' .
q	reinforcement ratio; $q = \frac{f_{sy}}{k f'_c} \frac{p}{(1-p)}$.
Q	total compressive force in steel above the neutral axis.
\bar{Q}	non-dimensionalized form for Q .
Q'	moment of Q about neutral axis.
\bar{Q}'	non-dimensionalized form for Q' .
r	mean radius of section.
R	strain ratio; $R = \frac{e_s}{e_{sy}}$.
S	total tensile force in steel below the neutral axis.
\bar{S}	non-dimensionalized form for S .
S'	moment of S about the neutral axis.
\bar{S}'	non-dimensionalized form for S' .
α	angle defining position of neutral axis.
θ	variable angle defining a typical point on the mean circumference; measured at the geometric centre from the point of maximum compressive strain.
θ_3	angle defining point on mean circumference at which $e_c = e'_c$.
θ_4	angle defining point on mean circumference above the neutral axis at which $e_s = e_{sy}$.
θ_5	angle defining point below the neutral axis at which $e_s = e_{sy}$.

3. Ultimate Strength Equations

3.1. Stress-Strain Relations

Experimental studies [4] have shown that the stress-strain relation for concrete under short-term compressive loading consists of an initial, relatively straight portion, in which stress is almost linearly proportional to strain, followed at higher stresses by a curved portion in which the slope decreases at an increasingly rapid rate. At the maximum stress, f'_c , the curve is horizontal. It then enters a final descending branch with decreasing stress but increasing strain, as shown in Fig. 1.

Although the criterion for final crushing of the concrete appears to be connected with the overall stability of the member [5], it is commonly assumed that, in members subjected to pure bending or combined bending and compression, concrete crushes at a limiting strain value. In the ACI Building Code [6], for example, the maximum strain in the extreme compression fibre at ultimate strength is given as 0.003.

In the present analysis the actual concrete stress-strain relation in compression will be idealized to that of an elastoplastic material. Fig. 1 shows the initial elastic region extending to the point represented by a maximum stress

Seite / page

fehlt /
manque /
missing

$$\cos \theta_3 = \cos \alpha + \frac{e'_c}{e_{cu}} \left(1 - \cos \alpha + \frac{t}{2r} \right), \quad (2)$$

$$\cos \theta_4 = \cos \alpha + \frac{e_{sy}}{e_{cu}} \left(1 - \cos \alpha + \frac{t}{2r} \right). \quad (3)$$

For relatively small values of eccentricity e , the tensile strain e_{s2} may remain smaller than e_{sy} so that no tensile yielding of the steel occurs. With larger eccentricities, such that

$$R = \frac{e_{s2}}{e_{sy}} \geq 1.0$$

the point below the neutral axis at which the steel tensile strain is equal to e_{sy} is defined by the angle θ_5 ,

$$\cos \theta_5 = \cos \alpha - \frac{e_{sy}}{e_{cu}} \left(1 - \cos \alpha + \frac{t}{2r} \right). \quad (4)$$

3.3. Equilibrium

The stress distributions in the steel and concrete at failure are shown in Fig. 2 for the condition $R > 1.0$. With the wall thickness t assumed to be small in comparison with the radius r , the concrete stress may be expressed as a function of the variable angle θ ,

$$\begin{aligned} f_c &= k f'_c && \text{for } 0 \leq \theta \leq \theta_3, \\ &= k f'_c \frac{\cos \theta - \cos \alpha}{\cos \theta_3 - \cos \alpha} && \text{for } \theta_3 \leq \theta \leq \alpha. \end{aligned}$$

In any small radial element above the neutral axis which subtends an angle $d\theta$ at the geometric centre, the concrete area is $(1-p)rt d\theta$. The compressive force acting on this element of concrete area is

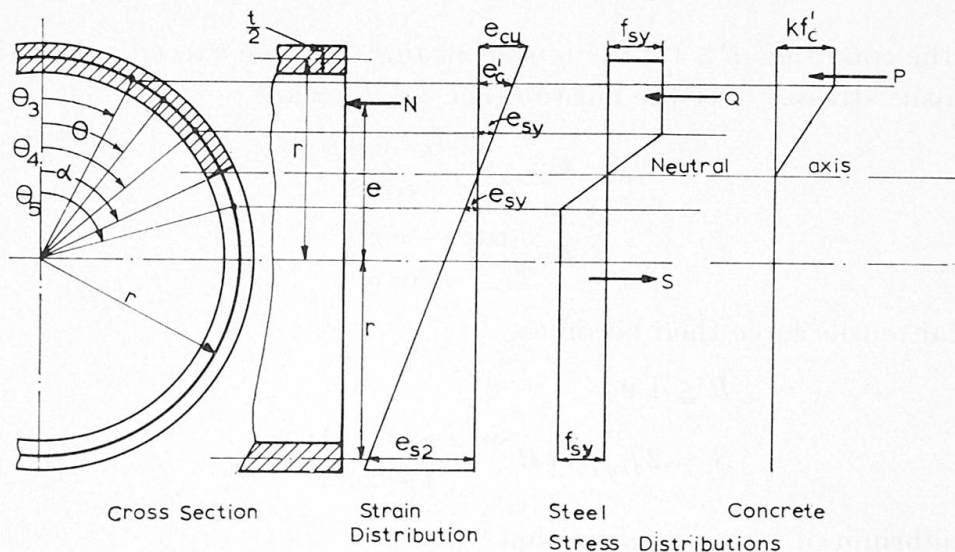


Fig. 2. Stress and strain distributions at ultimate load.

$$dP = f_c(1-p)rt d\theta. \quad (6)$$

The total compressive force in the concrete above the neutral axis is then

$$P = 2 \int_{\theta=0}^{\theta_3} k f'_c (1-p) r t d\theta + 2 \int_{\theta=\theta_3}^{\alpha} k f'_c \frac{\cos \theta - \cos \alpha}{\cos \theta_3 - \cos \alpha} (1-p) r t d\theta,$$

i. e.
$$P = 2 k f'_c (1-p) r t \left[\theta_3 + \frac{\sin \alpha - \sin \theta_3 - (\alpha - \theta_3) \cos \alpha}{\cos \theta_3 - \cos \alpha} \right]. \quad (7)$$

The compressive steel stresses are

$$\begin{aligned} f_s &= f_{sy} && \text{for } 0 \leq \theta \leq \theta_4, \\ &= f_{sy} \frac{\cos \theta - \cos \alpha}{\cos \theta_4 - \cos \alpha} && \text{for } \theta_4 \leq \theta \leq \alpha \end{aligned}$$

and the total compressive force in the steel becomes

$$Q = 2 f_{sy} p r t \left[\theta_4 + \frac{\sin \alpha - \sin \theta_4 - (\alpha - \theta_4) \cos \alpha}{\cos \theta_4 - \cos \alpha} \right]. \quad (8)$$

For the condition in which the extreme tensile strain e_{s2} equals or exceeds e_{sy} , i. e. for $R \geq 1.0$, the tensile stresses in the steel below the neutral axis are

$$\begin{aligned} f_s &= f_{sy} \frac{\cos \alpha - \cos \theta}{\cos \alpha - \cos \theta_5} && \text{for } \alpha \leq \theta \leq \theta_5, \\ &= f_{sy} && \text{for } \theta_5 \leq \theta \leq \pi \end{aligned}$$

and the total tensile force in the steel is

$$S = 2 \int_{\theta=\alpha}^{\theta_5} f_{sy} p r t \frac{\cos \alpha - \cos \theta}{\cos \alpha - \cos \theta_5} d\theta + 2 \int_{\theta=\theta_5}^{\pi} f_{sy} p r t d\theta,$$

i. e. for $R \geq 1.0$,

$$S = 2 f_{sy} p r t \left[\pi - \theta_5 + \frac{\sin \alpha - \sin \theta_5 + (\theta_5 - \alpha) \cos \alpha}{\cos \alpha - \cos \theta_5} \right]. \quad (9)$$

For the condition $R \leq 1.0$ the tensile strains nowhere exceed e_{sy} , so that the steel tensile stresses over the entire range $\alpha \leq \theta \leq \pi$ are

$$\begin{aligned} f_s &= E_s e_{s2} \frac{\cos \alpha - \cos \theta}{1 + \cos \alpha}, \\ &= R f_{sy} \frac{\cos \alpha - \cos \theta}{1 + \cos \alpha}. \end{aligned}$$

The total tensile force then becomes,

for $R \leq 1.0$,

$$S = 2 f_{sy} p r t R \frac{\sin \alpha + (\pi - \alpha) \cos \alpha}{1 + \cos \alpha}. \quad (9a)$$

Equilibrium of forces requires that

$$N = P + Q - S. \quad (10)$$

This equation may be expressed in non-dimensional form as

$$\frac{N}{2k f'_c (1-p) r t} = \bar{P} + q(\bar{Q} - \bar{S}), \quad (11)$$

where
$$q = \frac{f_{sy}}{k f'_c} \frac{p}{(1-p)} \quad (12)$$

$$\bar{P} = \theta_3 + \frac{\sin \alpha - \sin \theta_3 - (\alpha - \theta_3) \cos \alpha}{\cos \theta_3 - \cos \alpha}, \quad (13)$$

$$\bar{Q} = \theta_4 + \frac{\sin \alpha - \sin \theta_4 - (\alpha - \theta_4) \cos \alpha}{\cos \theta_4 - \cos \alpha}. \quad (14)$$

For $R \geq 1.0$,

$$\bar{S} = \pi - \theta_5 + \frac{\sin \alpha - \sin \theta_5 + (\theta_5 - \alpha) \cos \alpha}{\cos \alpha - \cos \theta_5}; \quad (15)$$

but when $R \leq 1.0$,

$$\bar{S} = R \frac{\sin \alpha + (\pi - \alpha) \cos \alpha}{1 + \cos \alpha}. \quad (15a)$$

A second equilibrium equation is obtained by considering the moments of forces about the neutral axis of the section,

$$N(e - r \cos \alpha) = P' + Q' + S', \quad (16)$$

where P' , Q' and S' are, respectively, the moments of the forces P , Q and S .

To obtain an expression for P' , it is first noted that the lever arm of the small compressive force dP (Eq. (6)) is $r(\cos \theta - \cos \alpha)$, so that

$$dP' = f_c (1-p) (\cos \theta - \cos \alpha) r^2 t d\theta$$

$$\text{and } P' = 2 \int_{\theta=0}^{\theta_3} k f'_c (1-p) (\cos \theta - \cos \alpha) r^2 t d\theta + 2 \int_{\theta=\theta_3}^{\alpha} k f'_c (1-p) \frac{(\cos \theta - \cos \alpha)^2}{\cos \theta_3 - \cos \alpha} r^2 t d\theta.$$

Upon integration, the above expression becomes

$$P' = 2k f'_c (1-p) r^2 t \bar{P}', \quad (17)$$

in which the term \bar{P}' is the trigonometric relation

$$\begin{aligned} \bar{P}' = & \sin \theta_3 - \theta_3 \cos \alpha + \frac{(\alpha - \theta_3)(0.5 + \cos^2 \alpha) - 1.5 \sin \alpha \cos \alpha}{\cos \theta_3 - \cos \alpha} \\ & + \frac{-0.5 \sin \theta_3 \cos \theta_3 + 2 \cos \alpha \sin \theta_3}{\cos \theta_3 - \cos \alpha}. \end{aligned} \quad (18)$$

The moment Q' is likewise obtained from the integral

$$Q' = 2 \int_{\theta=0}^{\alpha} f_s p r^2 t (\cos \theta - \cos \alpha) d\theta$$

as
$$Q' = 2 f_{sy} p r^2 t \bar{Q}', \quad (19)$$

$$\begin{aligned} \text{in which } \bar{Q}' = & \sin \theta_4 - \theta_4 \cos \alpha + \frac{(\alpha - \theta_4)(0.5 + \cos^2 \alpha) - 1.5 \sin \alpha \cos \alpha}{\cos \theta_4 - \cos \alpha} \\ & + \frac{-0.5 \sin \theta_4 \cos \theta_4 + 2 \cos \alpha \sin \theta_4}{\cos \theta_4 - \cos \alpha}. \end{aligned} \quad (20)$$

In obtaining an expression for the moment S' , two possible ranges of values for the ratio R must be considered. When $R \geq 1.0$, the tensile steel has yielded in the region $\theta_5 \leq \theta \leq \pi$, and so

$$S' = 2 \int_{\theta=\alpha}^{\theta_5} f_{sy} p r^2 t \frac{(\cos \alpha - \cos \theta)^2}{\cos \alpha - \cos \theta_5} d\theta + 2 \int_{\theta=\theta_5}^{\pi} f_{sy} p r^2 t (\cos \alpha - \cos \theta) d\theta.$$

The equation for S' then becomes

$$S' = 2 f_{sy} p r^2 t \bar{S}', \quad (21)$$

in which

$$\begin{aligned} \bar{S}' = & (\pi - \theta_5) \cos \alpha + \sin \theta_5 + \frac{(\theta_5 - \alpha)(0.5 + \cos^2 \alpha) + 1.5 \sin \alpha \cos \alpha}{\cos \alpha - \cos \theta_5} \\ & + \frac{+0.5 \sin \theta_5 \cos \theta_5 - 2 \cos \alpha \sin \theta_5}{\cos \alpha - \cos \theta_5}. \end{aligned} \quad (22)$$

When $R \leq 1.0$, the steel stress remains in the elastic range so that

$$S' = 2 \int_{\theta=\alpha}^{\pi} R f_{sy} p r^2 t \frac{(\cos \alpha - \cos \theta)^2}{\cos \alpha - \cos \theta_5} d\theta.$$

Integration of this expression yields

$$S' = 2 f_{sy} p r^2 t \bar{S}',$$

which is identical to Eq. (21), however in this case

$$\bar{S}' = R \frac{(\pi - \alpha)(0.5 + \cos^2 \alpha) + 1.5 \sin \alpha \cos \alpha}{(1 + \cos \alpha)}. \quad (22a)$$

Eq. (16) may now be written in non-dimensional form as

$$\frac{e}{r} = \cos \alpha + \frac{\bar{P}' + q(\bar{Q}' + \bar{S}')}{\bar{P}' + q(\bar{Q}' - \bar{S}')}. \quad (23)$$

It will be noted that the term q , defined in Eq. (12), is essentially a non-dimensional measure of the quantity of reinforcement in the cross-section. The terms \bar{P} , \bar{Q} , \bar{S} , \bar{P}' , \bar{Q}' and \bar{S}' , which all appear in Eq. (23), are non-dimensional trigonometric functions of the angles α , θ_3 , θ_4 and θ_5 . When $R \geq 1.0$ the terms \bar{S}' and \bar{S} are obtained from Eqs. (22) and (15), however when $R \leq 1.0$ Eqs. (22a) and (15a) are applicable. Equations for the other trigonometric expressions are *not* affected by the value of R .

The above equations may be used to evaluate the load N which, at eccentricity e , will cause failure of a thin-wall circular section. A trial value of α is

chosen, i. e. of the position of the neutral axis, and the angles θ_3 , θ_4 and θ_5 are evaluated, and thence e . The correct value for α has been chosen when this computed value for e is equal to the actual value. With the correct α found by trial and error, the force N can be evaluated.

4. Ultimate Strength Design

4.1. Design Charts

The procedure outlined at the end of the previous section for calculating the ultimate load N would in practice prove to be time consuming and tedious. The non-dimensional form in which the equations have been developed is however suitable for the preparation of design curves which can very much simplify and shorten the design procedure.

Eq. (23) is first rewritten as

$$\frac{e}{r} = \cos \alpha + \frac{C + qD}{A + qB} \quad (24)$$

in which

$$A = \bar{P}, \quad (25)$$

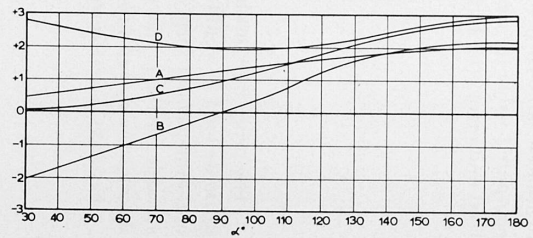
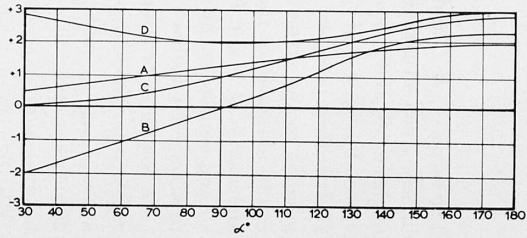
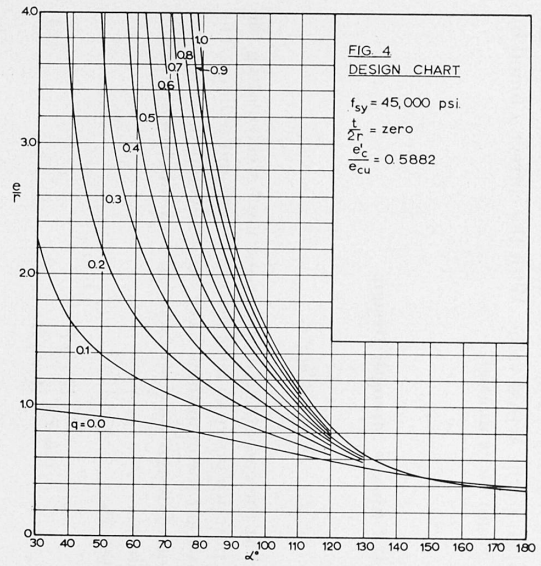
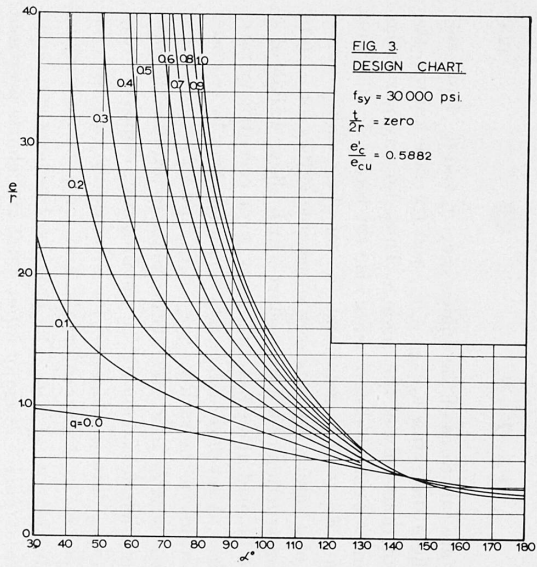
$$B = \bar{Q} - \bar{S}, \quad (26)$$

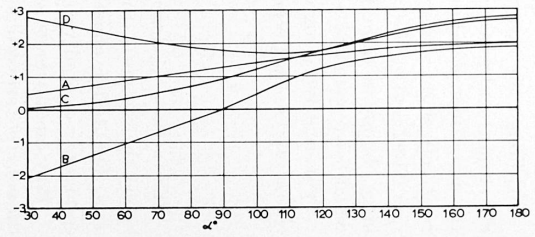
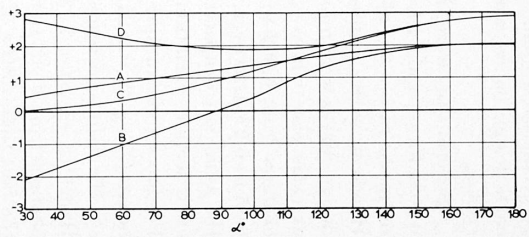
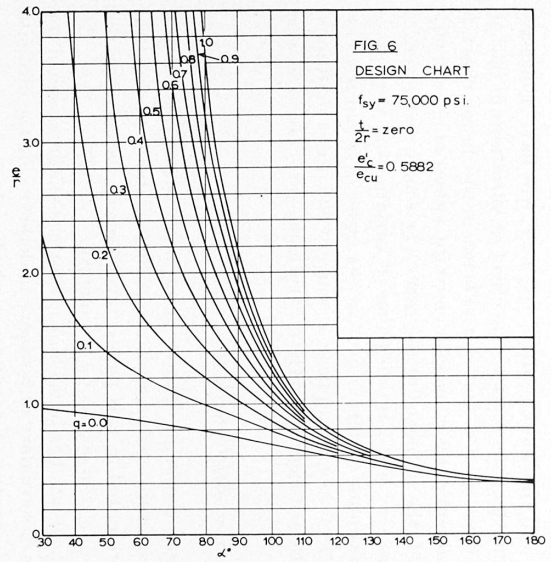
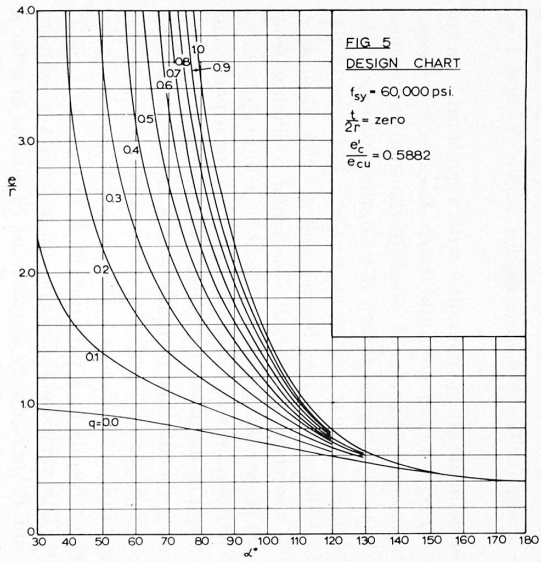
$$C = \bar{P}', \quad (27)$$

$$D = \bar{Q}' + \bar{S}'. \quad (28)$$

The terms A , B , C and D are functions of the angles α , θ_3 , θ_4 and θ_5 . However, in any given situation where the ratios e_{sy}/e_{cu} , e'_c/e_{cu} and $t/2r$ are known, the angles θ_3 , θ_4 and θ_5 are functions only of the angle α . Thus, for any particular value of α , θ_3 , θ_4 and θ_5 can be evaluated and hence also the terms A , B , C and D . It is then possible, using Eq. (24), to determine the set of e/r values corresponding to any given set of q values. By choosing successive values for α , data can be obtained for the construction of a design chart which allows values of α , and also A , B , C and D , to be read immediately for any given eccentricity ratio e/r and reinforcement ratio q . A set of design charts would however be required to allow for possible variations in the ratios e_{sy}/e_{cu} , e'_c/e_{cu} and $t/2r$.

A computer program was written in Fortran II language to produce the data required for the plotting of such design charts. In the program, values are read in for e'_c , e_{cu} , e_{sy} and $t/2r$ and data is generated for α values varying between 30 degrees and 180 degrees in 10 degree intervals, and for q values varying between zero and 1.0 in increments of 0.05. The program has been run on an IBM 1620 computer for an extensive range of input data, and charts prepared from four such runs are presented in Figs. 3 to 6.





4.2. Effect of Ratio $t/2r$

Although the ratio of wall thickness to diameter, $t/2r$, will have a decisive effect on the ultimate strength of the section, the effect of variations in $t/2r$ on the non-dimensional quantities A , B , C and D , and hence in the design chart, is relatively slight. In several computer runs with constant values of $e_{sy} = 0.001$, $e'_c = 0.002$ and $e_{cu} = 0.0034$, the influence of the ratio $t/2r$ was investigated. A large change in value from zero to 0.2 produced small variations in the curves which correspond to a maximum variation in N of the order of seven percent.

This relatively slight effect does not appear to warrant the use of additional charts, and in the preparation of Figs. 3 to 6 the $t/2r$ ratio has been taken as zero.

4.3. Effect of Ratio e'_c/e_{cu}

The ratio e'_c/e_{cu} determines the shape of the concrete stress-strain relation and hence the shape of the concrete compressive stress block above the neutral axis. The design charts presented in this paper have been prepared using the commonly quoted values of $e'_c = 0.002$ and $e_{cu} = 0.0034$.

Previous ultimate strength studies have shown that the shape assumed for the concrete stress block is of secondary importance in determining the ultimate load for "tension" type failures, i. e., for failures in which yielding occurs in the steel in the extreme tension fibres. In thin-walled bridge pier design the eccentricity ratio will usually be sufficiently large to ensure a tension type failure. Nevertheless, a small region has been included on the extreme right hand side of each design chart, where α approaches 180 degrees, for which $R < 1.0$, i. e., $e_{s2} < e_{sy}$.

Several runs were therefore made on the computer with a constant value of 0.0034 for e_{cu} and with e'_c varying between 0.001 and 0.002. As expected, increases in the ratio e'_c/e_{cu} did not have any significant effect for the smaller α values. However, with α values sufficiently large to ensure $R < 1.0$, the positions of the design curves were found to be sensitive to variations in e'_c/e_{cu} . For a particular extreme case where $f_{sy} = 30000$ psi, $\alpha = 180$ degrees and $q = 0.5$, then as e'_c changes from 0.002 to 0.001 the eccentricity ratio was found to change from 0.35 to 0.27. However we are more concerned with the change in magnitude of the axial force capacity N . It can be seen from Eq. (29) that for a particular cross-section, variation of N can be measured by variation of the term $(A + qB)$. For the above example when $e'_c = 0.002$, then from Fig. 3, $A = 2.04$ and $B = 2.40$, hence $(A + qB) = 3.24$. As a comparison, with the same values for f_{sy} , q and e/r , the values corresponding to $e'_c = 0.001$ are $\alpha = 150^\circ$, $A = 2.22$ and $B = 2.13$. Hence $(A + qB) = 3.28$, which results in a variation in N of only 0.1% as e'_c changes from 0.002 to 0.001. This very slight effect on ultimate load arises from the fact that values of A and B are not very sensitive to variations in α for α values approaching 180 degrees.

It is therefore concluded that, even in the extreme situations considered above, preparation of additional design charts for variations in e'_c/e_{cu} is not warranted.

4.4. Design Procedure

Under normal circumstances, the bridge superstructure will have been previously designed, and the worst combinations of axial loads and transverse and longitudinal moments due to dead and live loads will be known. The design of the pier proceeds by a trial and error procedure in which a section is chosen and then checked for adequate strength. The total axial force and the resultant of the transverse and longitudinal moments are calculated for the trial section and multiplied by the appropriate load factors.

The eccentricity ratio e/r and the reinforcement ratio

$$q = \frac{f_{sy} p}{k f'_c (1 - p)}$$

are then evaluated. The correct values of A and B for the trial section are then obtained directly from the appropriate design chart. It is to be noted that each design chart presented in this paper has been prepared for a particular steel yield stress. The four charts contained in Figs. 3 to 6 thus allow calculations to be made for reinforcing steels with yield stresses of from 30,000 psi to 75,000 psi. A value of 30×10^6 psi has here been assumed for the modulus of elasticity of the steel.

The ultimate load N is then calculated as

$$N = 2 k f'_c (1 - p) t r [A + q B]. \quad (29)$$

Provided the calculated ultimate load N exceeds the factored design load the section is safe.

The moment at failure can be found immediately from N as $N e$, however an independent check can be made using Eq. (30).

$$N e = 2 k f'_c (1 - p) t r^2 (C + q D) + N r \cos \alpha. \quad (30)$$

The design charts have been prepared for the following ranges of variables:

$$\begin{aligned} 30 &\leq \alpha \leq 180 \text{ degrees,} \\ 30,000 &\leq f_{sy} \leq 75,000 \text{ psi,} \\ 0 &\leq q \leq 1.0. \end{aligned}$$

Furthermore, only eccentricity ratios sufficiently large to ensure tension over part of the cross-sectional area, but less than 4.0, are considered. These ranges have been chosen to include all values which would normally be met with in bridge pier design.

4.5. Design Examples

To illustrate the use of the charts, calculations are made to determine the ultimate strength of two hollow circular bridge pier sections. Both sections had been designed previously on the basis of permissible stresses using the elastic analysis contained in Reference [2]. The results of the elastic analysis, which will allow an estimation to be made of the load factor against failure, are presented in the following table, together with cross-section details.

	Example A	Example B
Design Load	625 k.	1,087 k.
Design Moment	11,780 k. in	90,700 k. in
f_{ca}	1,350 psi	1,350 psi
f_{sa}	18,000 psi	30,000 psi
f_{cw}	1,240 psi	1,280 psi
f_{sw}	1,790 psi	18,000 psi
$k f_c'$	3,000 psi	3,000 psi
f_{sy}	30,000 psi	60,000 psi
n	10.0	10.0
r	33.5 in	62.5 in
t	5.0 in	7.0 in
e/r	0.563	1.34
p	0.010	0.014

In Example A the reinforcement ratio is computed as $q = 0.101$. It is assumed that the same load factor applies both to horizontal and vertical loads, i. e. to the axial force and bending moment, so that, at failure, the eccentricity ratio remains $e/r = 0.563$. On entering the design chart in Fig. 3 with the above values for q and e/r one obtains the values $\alpha = 130$ degrees and hence $A = 1.75$, $B = 1.56$. The ultimate load is then calculated from Eq. (29) as

$$N = 2 \times 3000 \times (1 - 0.01) \times 5 \times 33.5 [1.75 + 0.101 \times 1.56] = 1,900 \text{ kips.}$$

The load factor in this case is therefore $1900/625 = 3.05$.

In Example B the reinforcement ratio is computed as $q = 0.284$, and with $e/r = 1.34$, the values $A = +1.15$, $B = -0.3$ are read directly from Fig. 5. The ultimate load is thus

$$N = 2 \times 3000 \times (1 - 0.014) \times 7 \times 62.5 [1.15 + 0.284(-0.3)] = 2,750 \text{ kips,}$$

which gives a load factor of $2750/1087 = 2.53$.

5. Concluding Remarks

Information has been presented in this paper to facilitate the design of thin-wall circular reinforced concrete bridge piers by the ultimate strength method. Consideration has been given only to the ultimate load of sections

subjected to combined compression and moment, consequently problems such as instability, additional moment due to lateral deflection, etc., have not been taken into account in the preparation of the design charts. The question of appropriate load factors also has not been discussed, since code values vary considerably from country to country.

6. Acknowledgements

The work described in this paper was carried out in the Civil Engineering School of the University of New South Wales, Sydney, Australia. The computer program was run on the IBM 1620 installation at the Institute of Highway and Traffic Research of the University.

7. References

1. M. MADISON: Slip Forming New York State World's Fair Pavilion. *Journal American Concrete Institute*, Proc. Vol. 61, July, 1964.
2. ACI Committee 505 Report: Specification for the Design and Construction of Reinforced Concrete Chimneys. *Journal American Concrete Institute*. Proc. Vol. 51, Sept. 1954.
3. G. WINTER, L. C. URQUHART, C. E. O'ROURKE: Design of Concrete Structures. McGraw Hill, New York, 7th Ed., 1964, p. 87.
4. H. RÜSCH: Researches Toward a General Flexural Theory for Structural Concrete. *Journal American Concrete Institute*, Proc. Vol. 57, July, 1960.
5. A. P. KABAILA: Discussion of paper entitled: Load-Moment-Curvature Characteristics of Reinforced Concrete Cross-Sections by E. O. Pfrang, C. P. Siess and M. A. Sozen. *Journal American Concrete Institute*. Proc. Vol. 62, March, 1965.
6. ACI Standard 318-63: Building Code Requirements for Reinforced Concrete. ACI Publication, 1964.

Summary

Ultimate strength equations are presented for the analysis and design of thin-wall circular reinforced concrete bridge piers. The equations have been incorporated in a computer program which has been used to generate data for the plotting of design charts. Four such design charts, presented in the paper, greatly facilitate the design procedure.

Résumé

Des équations basées sur le calcul plastique sont présentées pour le dimensionnement des piles de pont circulaires à parois minces en béton armé. Ces équations ont été programmées pour être traitées par un ordinateur qui a

établi les données nécessaires à l'exécution d'abaques de calcul. Quatre de ces abaques, présentés ici, facilitent grandement le dimensionnement.

Zusammenfassung

Gleichungen für die Bemessungen von dünnwandigen, kreisförmigen Brückenfeilern nach dem Traglastverfahren werden aufgestellt.

Mit Hilfe einer elektronischen Rechenmaschine wurden Berechnungen durchgeführt, die für das Aufzeichnen von Bemessungskurven benutzt wurden. Vier Bemessungskurven werden vorgelegt, die die Bemessung von solchen Brückenfeilern beträchtlich vereinfachen.